



*J. Serb. Chem. Soc.* 86 (4) 415–427 (2021)  
JSCS–5431

## Synthesis of BaTi<sub>5</sub>O<sub>11</sub> by an aqueous co-precipitation method *via* a stable organic titanate precursor

PELIN SÖZEN AKTAŞ\*

*Manisa Celal Bayar University, Faculty of Arts & Sciences, Department of Chemistry,  
Şehit Prof. Dr. İlhan Varank Campus 45140 Muradiye-Manisa, Turkey*

(Received 6 July 2020, revised 10 February, accepted 17 February 2021)

**Abstract:** BaTi<sub>5</sub>O<sub>11</sub> has been widely researched due to its unique microwave properties. Conventionally, it is challenging to obtain this compound as a single phase. The BaTi<sub>5</sub>O<sub>11</sub> was synthesized *via* a co-precipitation technique using an aqueous solution of titanium(IV)(triethanolaminate) isopropoxide, barium nitrate and ammonia as precursors, which are stable in aqueous media. The phase evolution, purity, and structure were identified by X-ray diffraction (XRD), scanning electron microscopy (SEM) and energy dispersive X-ray (EDX) spectroscopy analysis. The desired BaTi<sub>5</sub>O<sub>11</sub> structure was obtained by calcination at 900 °C. Furthermore, the structure was characterized by TGA, FT-IR and Raman studies. The study showed that the particles were between 80 and 120 nm in size and the average crystallite size was determined from the Scherrer formula as 68.1 nm at 900 °C.

**Keywords:** barium titanium oxide system; organic titanate; co-precipitation; X-ray diffraction.

### INTRODUCTION

Electronic components and other ceramic substrates have been investigated intensively due to the rapid growth of high-frequency wireless communication technology.<sup>1</sup> Low-temperature co-firing ceramic (LTCC) technology is of great interest today to manufacture miniaturized multilayer devices with diverse functions.<sup>2</sup> By utilizing this technology, multi-chip packages have been successfully synthesized using a single sheet to construct and integrate the appropriate electronic components and devices in a compact multi-layered ceramic architecture. After laminating, the sintering temperature should be chosen to be below 1000 °C to use low resistance conductors, such as gold and silver. In this way, rapid signal transmission between modules with high conductivity and energy loss is minimized. LTCC materials are generally preferred for applications such as dual-

\* E-mail: pelin.sozen@cbu.edu.tr  
<https://doi.org/10.2298/JSC200706014A>

band baluns, bandpass filters, power distribution networks, point-to-point transceivers (passive elements) and voltage-controlled oscillators, dielectric resonator oscillators, amplifiers and singly balanced mixers.<sup>3</sup> To date, many LTCC materials have been developed and intensively applied, including BiNbO<sub>4</sub>, MTiO<sub>3</sub> (M = Mg, Zn, Ca), BaO–TiO<sub>2</sub>, ZnNb<sub>2</sub>O<sub>6</sub>, BaO–R<sub>2</sub>O<sub>3</sub>TiO<sub>2</sub> (R = Nd, Sm) and Li<sub>1+x-y</sub>Nb<sub>1-x-3y</sub>Ti<sub>x+4y</sub>O<sub>3</sub>, *etc.*<sup>2</sup> Among these, compounds in the binary system of BaO–TiO<sub>2</sub> have been accurately reported to undoubtedly possess excellent microwave properties. BaTi<sub>5</sub>O<sub>11</sub> has been researched for use in microwave applications considering its superior properties.<sup>4-7</sup> Zhou and co-workers reported that BaTi<sub>5</sub>O<sub>11</sub> synthesized at 1100 °C with CuO addition showed excellent microwave dielectric properties. BaTi<sub>5</sub>O<sub>11</sub> exhibited a dielectric constant ( $\epsilon_r$ ) of 41.2, a  $Qf$  of 47430 GHz ( $Q$  is the quality factor and  $f$  is the resonant frequency) and a temperature coefficient ( $\tau_f$ ) of 36 ppm °C<sup>-1</sup>.<sup>8</sup> Sintering of BaTi<sub>5</sub>O<sub>11</sub> ceramic with 4 wt. % Ba–ZnO and B<sub>2</sub>O<sub>3</sub> (BZB glass) at 900 °C was also reported, and these ceramics demonstrated excellent dielectric properties, that is  $\epsilon_r = 35.36$  and  $Qf = 28095$  GHz.<sup>9</sup> As wireless communication systems require an LTCC that has been sintered at temperatures below 1000 °C, BaTi<sub>5</sub>O<sub>11</sub> could be enthusiastically recommended as a suitable material candidate for application in microwave ceramic components.

BaTi<sub>5</sub>O<sub>11</sub> was first synthesized by Tillmanns, but the preparation method was not a single-phase process.<sup>10</sup> Afterwards, BaTi<sub>5</sub>O<sub>11</sub> was obtained by a solid-state reaction in the 1970s as an intermediate.<sup>11</sup> A single-phase BaTi<sub>5</sub>O<sub>11</sub> structure could be prepared by chemical processes, such as co-precipitation, sol–gel, hydrothermal, and alkoxide-derived powder sintering.<sup>6,12-15</sup> BaTi<sub>5</sub>O<sub>11</sub> was synthesized at calcination temperatures between 700 and 1100 °C by using alkoxide and sol–gel methods.<sup>6,16,17</sup> On the other hand, single-phase synthesis studies in powder form are currently under investigation using different ways. High-quality powder of BaTi<sub>5</sub>O<sub>11</sub> was obtained by co-precipitation using BaCl<sub>2</sub> and TiCl<sub>4</sub> as the starting materials.<sup>18</sup> In most cases, these kinds of Ti precursors are moisture sensitive and must be protected from rapid hydrolysis.

In the present study, BaTi<sub>5</sub>O<sub>11</sub> powder was synthesized in an aqueous solution by co-precipitation processing. The starting materials are stable in an aqueous environment and could be efficiently prepared on an industrial scale. It also offers the possibility to work with low temperatures (at 900 °C) and commercially available inexpensive starting materials.

## EXPERIMENTAL

### *Materials and method*

Barium nitrate (>99 % purity, Sigma Aldrich), titanium (triethanolaminato) isopropoxide solution (80 wt. % in isopropanol, Sigma Aldrich), nitric acid (HNO<sub>3</sub>, 65 wt. % and NH<sub>3</sub>, 25 wt. %, Isolab) were used as the starting materials. The obtained calcined powders were characterized by X-ray diffraction (XRD) on a PANalytical Empyrean diffractometer with Cu

$K\alpha$  radiation ( $\lambda = 1.5406 \text{ \AA}$ ) with a scan speed of  $0.05^\circ \text{ s}^{-1}$ , in the  $2\theta$  range from 10 to  $80^\circ$ . Match! version 3 crystal impact was used for phase identification and composition.<sup>19</sup> The X-ray pattern of the sample calcined at  $900^\circ \text{C}$  was analyzed by the Rietveld refinement program FULLPROF using the data obtained at  $1^\circ \text{ min}^{-1}$  scan rate in the  $20\text{--}70^\circ 2\theta$  range.<sup>20</sup> The crystal structure was pictured by the VESTA program.<sup>21</sup> FTIR spectra of the samples were recorded on Spectrum BX Perkin Elmer FT-IR spectrometer using KBr pellets. Spectragryph Software for optical spectroscopy Version 1.2.13 was used to create multi-spectrum plots.<sup>22</sup> For Raman analysis, Renishaw Invia Raman System equipped with a Leica model confocal microscope and an Argon-ion laser light source (532 nm) and  $50\times$  objective was used. Thermogravimetric analysis was performed on a SII 7300 Perkin Elmer thermal analyzer under flowing  $\text{N}_2$  at  $2.5 \text{ mL min}^{-1}$  from 25 to  $1200^\circ \text{C}$  at a heating rate of  $5^\circ \text{C min}^{-1}$ . Scanning electron microscopy (SEM) was used to analyze the morphology of the synthesized  $\text{BaTi}_5\text{O}_{11}$  structure. SEM images were taken by a Zeiss Gemini 500 microscope. The average particle diameters were measured from each SEM image. Energy-dispersive X-ray spectroscopy (EDX) was used to ascertain the chemical composition of the material.

#### Preparation of $\text{BaTi}_5\text{O}_{11}$

The  $\text{BaTi}_5\text{O}_{11}$  powders were prepared by a simple co-precipitation process. A barium nitrate solution was prepared by dissolving  $\text{Ba}(\text{NO}_3)_2$  (4 mmol, 0.1054 g) in 20 mL ultrapure water. This solution was then added to an organic titanate mixture (20 mmol, 6.328 g, titanium (triethanolaminate) isopropoxide solution) in 80 mL of 1M  $\text{HNO}_3$  aqueous solution. The concentrations of  $\text{Ba}^{2+}$  and  $\text{Ti}^{4+}$  in the solution were 0.04 and 0.2 M, respectively. The mixture was stirred at room temperature for 1 h to obtain a pellucid solution (pH 1). The pH of the solution was adjusted to 9 by adding an aqueous 1 M ammonia solution. After precipitation was complete, the suspension was further stirred at  $50^\circ \text{C}$  for 2 h. The suspension was first cooled to room temperature then kept in a deep-freezer (about  $-20^\circ \text{C}$ ) for 1 h. The precipitate was filtered and washed with a small amount of cold ultrapure water and dried at  $80^\circ \text{C}$  in a vacuum oven. The resultant material was first calcined for 4 h at different temperatures ranging from 700 to  $1000^\circ \text{C}$  at a heating rate of  $5^\circ \text{C min}^{-1}$  in an alumina crucible. The synthesis route of the co-precipitation method is given in Fig. 1.

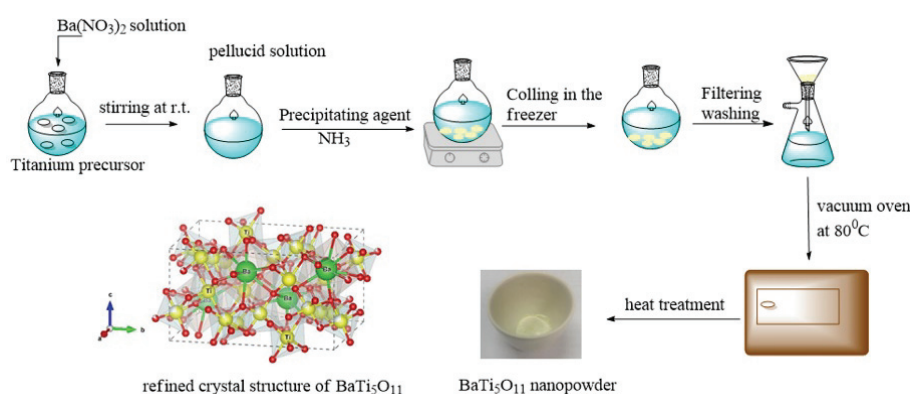
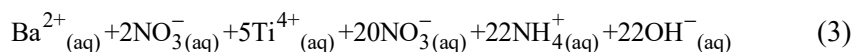
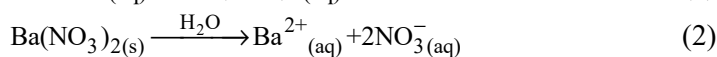
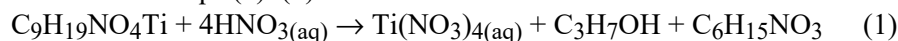


Fig. 1. Representation of the key steps of  $\text{BaTi}_5\text{O}_{11}$  synthesis *via* the proposed co-precipitation method.

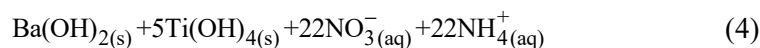
## RESULTS AND DISCUSSION

*Synthesis of BaTi<sub>5</sub>O<sub>11</sub>*

Preparation of large amounts of barium titanium oxide systems requires economic, air-stable starting precursors, high yields, aqueous media, and excellent reproducibility. The BaTi<sub>5</sub>O<sub>11</sub> system is challenging to prepare and is often synthesized as an intermediate product.<sup>11</sup> For this purpose, to obtain BaTi<sub>5</sub>O<sub>11</sub>, a simple synthetic route has been developed in an aqueous medium. The proposed reaction mechanism for the preparation of BaTi<sub>5</sub>O<sub>11</sub> by the co-precipitation method is shown in Eqs. (1)–(7):



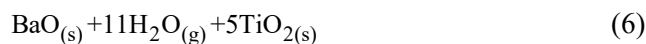
↓ co-precipitation



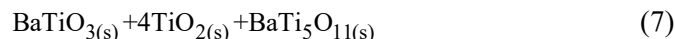
↓ filtration



↓ heat-treatment



↓



The mechanism for the co-precipitation reaction has been proposed considering similar studies using organic titanate.<sup>14,23</sup> Under acidic conditions, it may be regarded as that 2-propanol and triethanolamine are formed by the addition of 1 M HNO<sub>3</sub> to the titanium (triethanolaminato) isopropoxide solution in the first step (Eq. (1)). In the second step, precipitation was realized by addition of ammonia to the barium nitrate and acidic titanate solution. Ammonia (1 M) was added until pH 9 for complete precipitation as represented in Eq. (3). In the solution, the concentration of Ba<sup>2+</sup> was 0.04 M while that of Ti<sup>4+</sup> was 0.2 M before ammonia addition. The first species precipitated in the solution is a water-insoluble titanium hydroxide. Barium hydroxide is strongly basic and soluble in water. Using the cooling process for precipitation allowed the formation of barium hydroxide. Similar observations were detected in the precipitation reaction with 1 M NaOH using barium acetate and dihydroxybis(ammoniumlactato) titanium.<sup>14</sup>

After filtering, washing, and drying processes, the precipitate was calcined to different temperatures. The proposed mechanism is based on the XRD analysis of samples obtained from the calcination process and represented in Eq. (5)–(7).

XRD profile at 800 °C indicates that trace amounts of BaTiO<sub>3</sub> and TiO<sub>2</sub> formation. TiO<sub>2</sub> synthesis from titanium (triethanolaminato) isopropoxide solution in acidic media was reported by Kong *et al.*<sup>23</sup> At temperatures below 800 °C, it could be assumed that BaO and TiO<sub>2</sub>, as well as BaTiO<sub>3</sub>, are formed. In the next step, the BaTi<sub>5</sub>O<sub>11</sub> structure was obtained from BaTiO<sub>3</sub> and TiO<sub>2</sub> at 900 °C.

#### XRD analysis and rietveld refinement

The XRD powder patterns of the BaTi<sub>5</sub>O<sub>11</sub> precursors calcined at different temperatures are presented in Fig. 2. The XRD profiles show that the BaTi<sub>5</sub>O<sub>11</sub> structure started to form at 800 °C. In the sample calcined at 700 °C, the organic residues were not separated, and the structure of the barium titanium oxide system was not formed (Supplementary material to this paper, Fig. S-1). In the sample calcined at 800 °C, a three-phase mixture of BaTi<sub>5</sub>O<sub>11</sub> (64.6 wt. %, JCPDS No. 35-0805), TiO<sub>2</sub> (18.0 wt. %, JCPDS No. 21-1272) and BaTiO<sub>3</sub> (17.4 wt. %, JCPDS No. 79-2263) was observed. At 900 °C, BaTi<sub>5</sub>O<sub>11</sub> as a single-phase was formed. Song and co-workers reported similar observations. In the study, BaTi<sub>5</sub>O<sub>11</sub> was prepared from the precursors BaTiO<sub>3</sub> and TiO<sub>2</sub>.<sup>25</sup> The powder XRD pattern of the dried sample calcined at 1000 °C indicated partial decomposition of BaTi<sub>5</sub>O<sub>11</sub> giving a mixture of BaTi<sub>5</sub>O<sub>11</sub> (65.7 wt. %), BaTi<sub>4</sub>O<sub>9</sub> (8.1 wt. %, JCPDS No. 34-0070) and Ba<sub>4</sub>Ti<sub>13</sub>O<sub>30</sub> (26.2 wt. %, JCPDS No. 35-0750). In studies related to BaTi<sub>5</sub>O<sub>11</sub> synthesis, it was observed that the structure began to deteriorate, and second or third phases emerged. Javadpour *et al.*<sup>24</sup> reported the decomposition of BaTi<sub>5</sub>O<sub>11</sub> into Ba<sub>2</sub>Ti<sub>9</sub>O<sub>20</sub> and TiO<sub>2</sub>. Additionally, Tanguank *et al.*<sup>6</sup> and Song *et al.*<sup>25</sup> reported second and third phase formation.

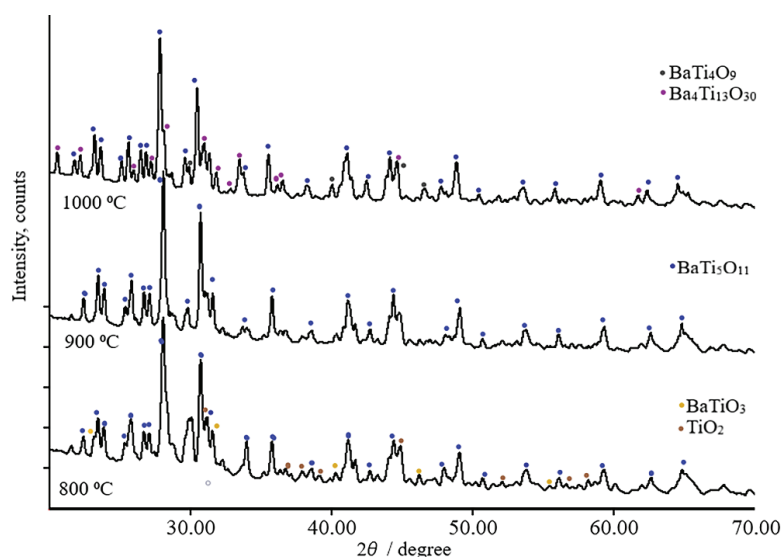


Fig. 2. Powder XRD patterns of dried samples calcined for 4 h at different temperatures.

Song and co-workers reported that in the temperature range below 900 °C, both  $\text{BaTi}_5\text{O}_{11}$  and  $\text{BaTi}_4\text{O}_9$  increased with calcination temperature and above 900 °C, the  $\text{BaTi}_5\text{O}_{11}$  content started to decrease, and the  $\text{BaTi}_4\text{O}_9$  content increased.<sup>25</sup>

The XRD results also showed well-defined diffraction peaks, and the major peaks were identified a monoclinic phase, indicating that  $\text{BaTi}_5\text{O}_{11}$  powders can be prepared by a simple co-precipitation method and heat treatment at 900 °C.

Since the single-phase  $\text{BaTi}_5\text{O}_{11}$  was obtained by calcination at 900 °C, this sample was chosen for Rietveld refinement (Fig. 3). The refinement parameters and the unit cell parameters are very compatible with data obtained by Tillmans *et al.*<sup>10</sup> The model provides a good fit between the observed and calculated X-ray diffraction profiles. A summary of the refinement and unit cell parameters for the  $\text{BaTi}_5\text{O}_{11}$  powder is interpreted in Table I, while atomic positions are given in Table II. The *R* factors show a reliable structural model. In the Rietveld refinement, the pseudo-Voigt function was used with standard Debye–Scherrer geometry to describe the peak shape. Since site occupancies obtained from the Rietveld refinement of  $\text{BaTi}_5\text{O}_{11}$  give  $\text{Ba}_{1.17}\text{Ti}_{4.785}\text{O}_{17.973}$  as the composition, it could wrongly be concluded that the oxygen content is increased by almost 70 %. This is actually a consequence of the great difference between the X-ray scattering powers of Ba and O atoms and hence this increase should not be considered as a real one.

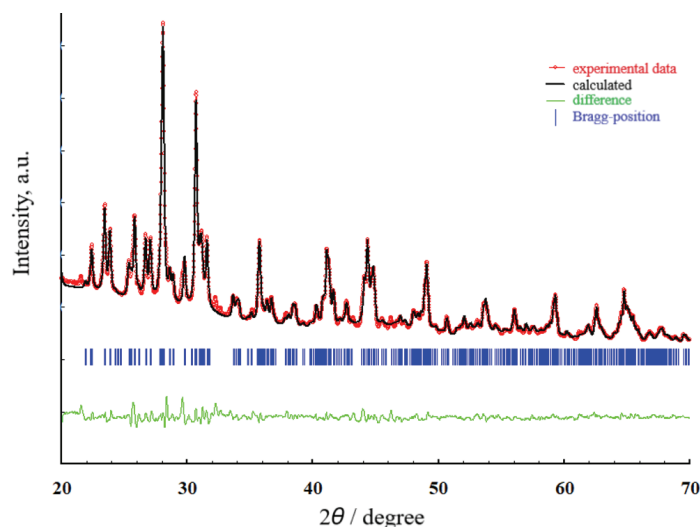


Fig. 3. Rietveld refinement of  $\text{BaTi}_5\text{O}_{11}$ .

The refined crystal structure of  $\text{BaTi}_5\text{O}_{11}$  is shown in Fig. 4. The unit cell contains four twelve-fold coordinated barium ions. Their bonding to the Ti octahedrons is realized through shared oxygen atoms. Twenty  $\text{Ti}^{4+}$  are ideally placed in the center of the octahedron formed by oxygen ions. The average crystallite

size estimated by the Scherrer formula was 68.1 nm at 900 °C, using the (140) diffraction peak.

TABLE I. Structure refinement parameters and crystal data for BaTi<sub>5</sub>O<sub>11</sub>

Formula: BaTi <sub>5</sub> O <sub>11</sub>
Formula weight: 552.66 g/mol
$T = 298$ K
$\lambda = 1.54060$ Å
Monoclinic crystal system, Space group – $P 1 2_1/n 1$ (#14)
Unit cell parameters: $a = 7.6670(3)$ Å; $b = 14.0410(3)$ Å; $c = 7.5325(3)$ Å; $\beta = 98.3710(2)^\circ$
Volume = 802.25 (1) Å <sup>3</sup>
$Z = 4$
Calculated Density = 4.588 g cm <sup>-3</sup>
$2\theta$ range = 10.0078–79.9922°; $2\theta$ step = 0.0131°
$\chi^2 = 2.60$ %; $R_F = 5.59$ %; $R_{\text{Bragg}} = 5.72$ %
$R_p = 12.7$ %; $R_{\text{wp}} = 13.9$ %; $R_{\text{exp}} = 8.59$ %

TABLE II. Atomic positions for BaTi<sub>5</sub>O<sub>11</sub> calcined at 900 °C for 4 h

Atom	Wyckoff position	$x$	$y$	$z$	Occupancy
Ba	4e	0.220 (3)	0.086 (3)	0.204 (3)	1.171 (3)
O1	4e	0.989 (3)	0.265 (3)	0.005 (3)	1.189 (2)
O2	4e	0.120 (3)	0.410 (3)	0.797 (3)	2.129 (2)
O3	4e	0.375 (3)	0.246 (3)	0.132 (3)	1.076 (2)
O4	4e	0.241 (3)	0.232 (3)	0.713 (3)	3.098 (2)
O5	4e	0.421 (3)	0.399 (3)	0.953 (3)	1.033 (2)
O6	4e	0.783 (3)	0.429 (3)	0.061 (3)	2.039 (2)
O7	4e	0.157 (3)	0.402 (3)	0.194 (3)	1.487 (2)
O8	4e	0.075 (3)	0.249 (3)	0.385 (3)	1.119 (2)
O9	4e	0.343 (3)	0.431 (3)	0.539 (3)	1.168 (2)
O10	4e	0.516 (3)	0.412 (4)	0.273 (3)	0.789 (2)
O11	4e	0.92 (3)	0.429 (3)	0.388 (3)	2.846 (1)
Ti1	4e	0.193 (3)	0.320 (4)	0.959 (3)	1.269 (2)
Ti2	4e	0.223 (3)	1.000 (3)	0.760 (3)	0.737 (2)
Ti3	4e	0.348 (3)	0.337 (4)	0.377 (3)	1.139 (2)
Ti4	4e	0.565 (3)	0.331 (4)	0.089 (3)	0.787 (2)
Ti5	4e	0.97 (3)	0.334 (4)	0.255 (3)	0.853 (2)

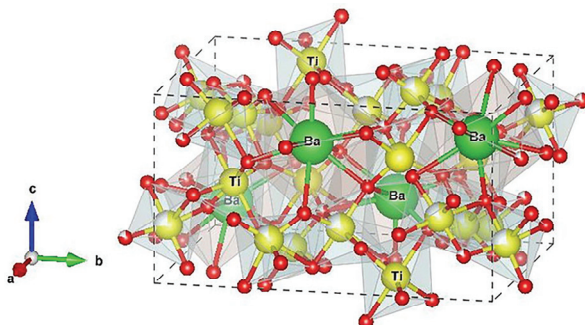


Fig. 4. Refined crystal structure of monoclinic BaTi<sub>5</sub>O<sub>11</sub>.



### TGA–DTG Analysis

The presented curves corresponding to the TGA and DTG analyses are given in Fig. 5. The first weight loss between 50 to 200 °C was attributed to the desorption of adsorbed water and light volatiles, such as 2-propanol, with a total loss of about 15 wt. %. The second weight loss up to 410 °C was due to dehydration and destruction of small organic residuals, which were also observed in the FT-IR spectrum of powder dried at 80 °C. The mass is almost stable above 410 °C. Finally, between 900 and 1000 °C, the powder weight remained at about 78 wt. % of the sample.

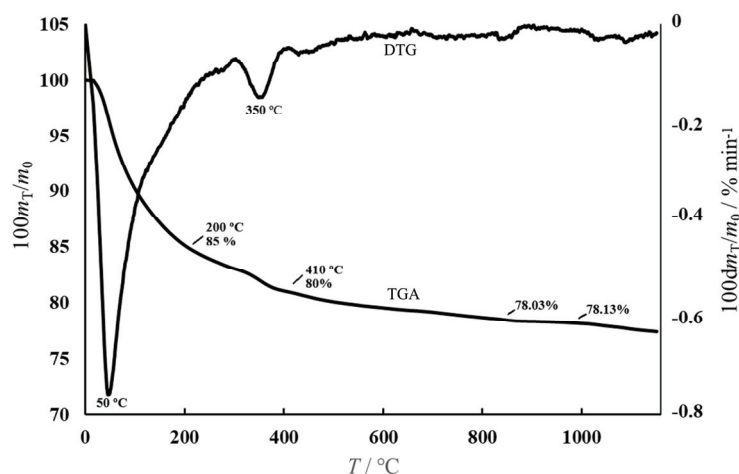


Fig. 5. TGA and DTG curves of the as-prepared BaTi<sub>5</sub>O<sub>11</sub> powders dried at 80 °C.

### FT-IR and Raman analysis

The phase identification of BaTi<sub>5</sub>O<sub>11</sub> powders synthesized by the homogeneous precipitation technique was further analyzed by FT-IR and Raman spectroscopy. The obtained FT-IR data was found to be consistent with the literature.<sup>6</sup> The IR spectra of the as-prepared and dried BaTi<sub>5</sub>O<sub>11</sub> powder calcined at different temperatures are shown in Fig. 6. The absorption peaks at 3819 (O–H stretching), 3443 (N–H asymmetric stretching), 1959 (C–H bending), 1628 (N–H bending), 1349 (NO<sub>3</sub><sup>-</sup> asymmetric stretching) and 1093 cm<sup>-1</sup> (NO<sub>3</sub><sup>-</sup> symmetric stretching) for the as-prepared sample at 80 °C correspond to the vibration modes of the functional groups of the starting precursors. After calcination of the dried powder, these characteristic peaks disappeared. At 800 °C, the peaks appear at 663, 556, 472 and 442 cm<sup>-1</sup>. These new bands below 800 cm<sup>-1</sup> support the formation of the BaTi<sub>5</sub>O<sub>11</sub> structure. The FTIR spectra of the BaTi<sub>5</sub>O<sub>11</sub> system have characteristic absorption peaks between 800–400 cm<sup>-1</sup>, and these are used to identify the phase formation.<sup>6,18</sup>



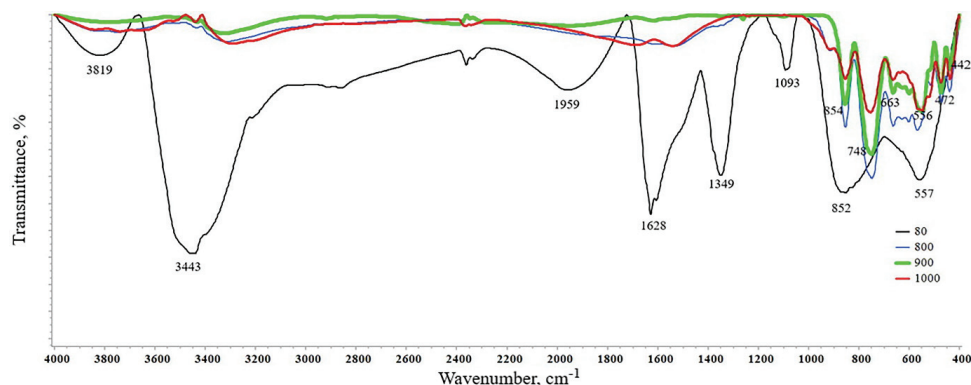


Fig. 6. FT-IR spectra of  $\text{BaTi}_5\text{O}_{11}$  calcined at different temperatures of as prepared precipitate dried at: 1) 80, 2) 800, 3) 900 and 4) 1000 °C.

The room temperature Raman spectrum of  $\text{BaTi}_5\text{O}_{11}$  obtained at 900 °C is shown in Fig. 7. The  $\text{BaTi}_5\text{O}_{11}$  sample prepared at 900 °C for 4 h showed characteristic peaks at 140, 194, 219, 243, 262, 294, 310, 343, 415, 487, 541, 590, 673, 747 and 835  $\text{cm}^{-1}$ , which confirmed that the material was pure. The analysis also indicated that the results agreed with those of Lu *et al.*<sup>16</sup>, Javadpour *et al.*<sup>24</sup> and Alvarez-Docio *et al.*<sup>4</sup> The Raman characterization for the thermally treated sample at 900 °C confirmed the formation of the  $\text{BaTi}_5\text{O}_{11}$  phase.

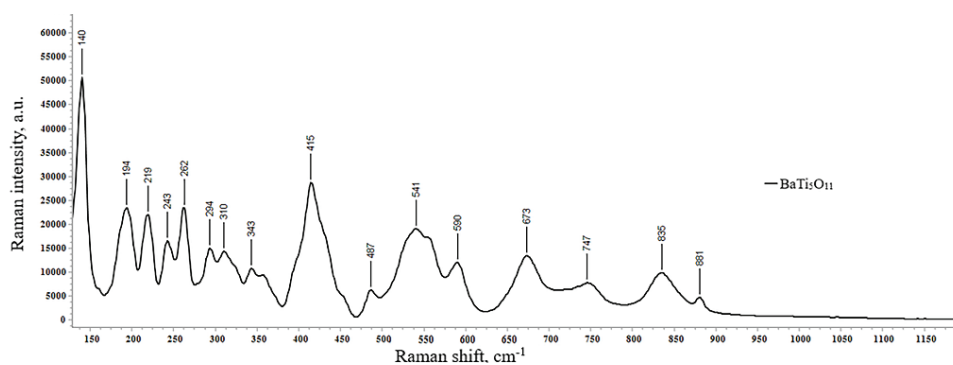


Fig. 7. Raman spectrum of the  $\text{BaTi}_5\text{O}_{11}$  synthesized by co-precipitation at 900 °C.

### SEM and EDX analysis

The morphologies of the  $\text{BaTi}_5\text{O}_{11}$  nanoparticles were studied by scanning electron microscopy. SEM micrographs of particles at 900 °C are shown in Fig. 8.

As seen in the SEM images, the synthesized  $\text{BaTi}_5\text{O}_{11}$  grains were in almost round shape and agglomerated. The particle sizes determined from the SEM images were between 80–120 nm. EDX analysis of particles calcined at 900 °C is given in Fig. 9 and confirmed the accuracy of the elemental composition. These

results demonstrate that the simple co-precipitation method is relatively useful for producing fine particles.

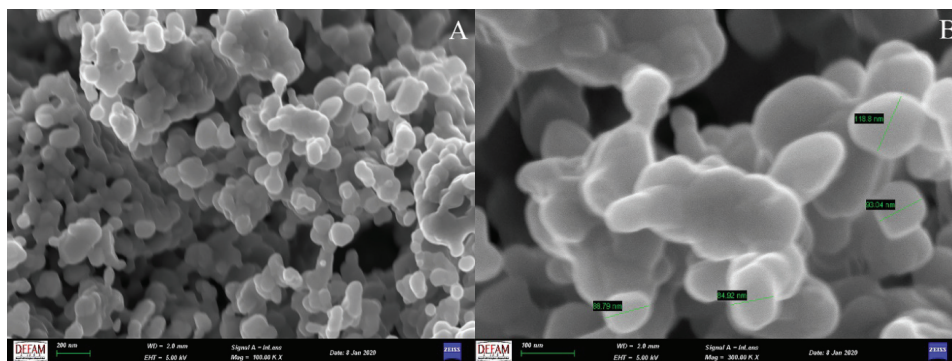


Fig. 8. SEM micrographs of  $\text{BaTi}_5\text{O}_{11}$  particles at  $900\text{ }^\circ\text{C}$  (A, B). Detected grain sizes from selected points (B: 84.92, 88.79, 93.04, 118.8 nm).

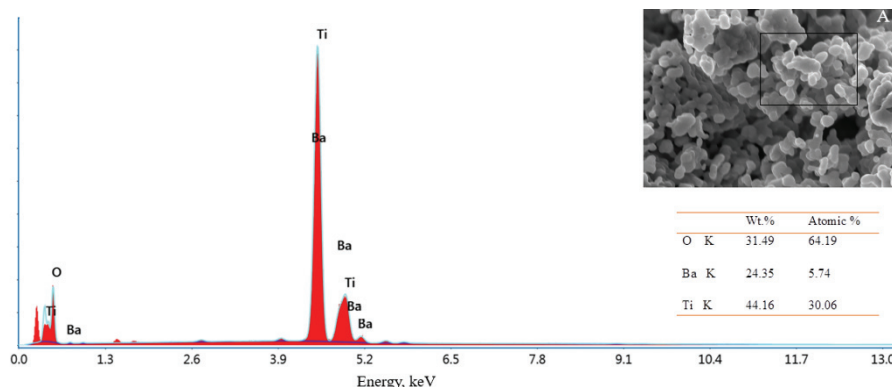


Fig. 9. EDX analysis of particles calcined at  $900\text{ }^\circ\text{C}$ .

#### *Comparison of results with literature data*

The synthesis processes of  $\text{BaTi}_5\text{O}_{11}$  are summarized in Table III (also corresponding literature are included for comparison).

In the present study,  $\text{BaTi}_5\text{O}_{11}$  of 80–120 nm particle size was synthesized from  $\text{Ba}(\text{NO}_3)_2$  and an organic titanate precursor. By comparing with other methods, this synthesis process demonstrated many advantageous properties such as low calcination temperature, lack of a minor second phase, and using economically inexpensive air-sensitive precursors. It could be considered for possible applications in LTCC systems due to its co-fired properties under  $1000\text{ }^\circ\text{C}$  by using electrodes such as Ag, Cu without high process temperatures, leading to energy consumption.

TABLE III. Experimental conditions for BaTi<sub>5</sub>O<sub>11</sub> prepared by various methods

Method	Precursors	Conditions	Morphology	Reference
Co-precipitation	Ba(NO <sub>3</sub> ) <sub>2</sub> organic titanate	4 h, 900 °C	80–120 nm (particle size)	In the present study
Co-precipitation	BaCl <sub>2</sub> ; TiCl <sub>4</sub>	4 h, 1100 °C	600 nm (particle size)	Tangjuank <i>et al.</i> <sup>18</sup>
Hydrothermal	Ba(CH <sub>3</sub> COO) <sub>2</sub> C <sub>6</sub> H <sub>18</sub> N <sub>2</sub> O <sub>8</sub> Ti	20 h, 280 °C	20–65 nm (particle size)	Liu <i>et al.</i> <sup>14</sup>
Alkoxide	Ba and Ti-isopropoxide	48 h, 1120 °C	1 μm (grain size)	Fukui <i>et al.</i> <sup>12</sup>
Solid-state <sup>a</sup>	BaCO <sub>3</sub> TiOCl <sub>2</sub>	10 days r.t. aging 1 min, 1000 °C	40–200 nm (grain size)	Álvarez-Docio <i>et al.</i> <sup>4</sup>
Citrate Route	Ba(NO <sub>3</sub> ) <sub>2</sub> TiCl <sub>4</sub>	4 h, 1100 °C	30–50 nm (particle size)	Choy <i>et al.</i> <sup>26</sup>

<sup>a</sup>Formation of BaTiO<sub>3</sub>, BaTi<sub>4</sub>O<sub>9</sub> intermediates

### CONCLUSIONS

In the present study, BaTi<sub>5</sub>O<sub>11</sub> nano powders were successfully synthesized by the co-precipitation method using commercially available, low-cost, and stable organic titanate complex of triethanolamine. This is also an advantageous feature when compared with other preferred synthesis methods. The reaction process is an effective method to synthesize the BaTi<sub>5</sub>O<sub>11</sub> structure for applications on low-temperature co-fired ceramics.

By using this newly developed secure method, a simple aqueous synthesis pathway was improved, and single-phase BaTi<sub>5</sub>O<sub>11</sub> powder was produced at 900 °C. TGA-DTG, FT-IR, and XRD analyses also confirmed that the nano powders were obtained at 900 °C. The average crystallite particle size was 68 nm, as determined by XRD. SEM analyses showed that these particles were agglomerated, almost round in shape, and with a size of 80–120 nm.

### SUPPLEMENTARY MATERIAL

Additional data are available electronically at the pages of journal website: <https://www.shd-pub.org.rs/index.php/JSCS/index>, or from the corresponding author on request.

*Acknowledgements.* This work was supported by the Scientific Research Project Office of Manisa Celal Bayar University, Project No: 2019-056. This paper's analyses were partially performed at Manisa Celal Bayar University (Turkey) – Applied Science and Research Center (DEFAM).

### ИЗВОД СИНТЕЗА BaTi<sub>5</sub>O<sub>11</sub> КОПРЕЦИПИТАЦИЈОМ ПОМОЋУ СТАБИЛНОГ ОРГАНСКОГ ТИТАНАТНОГ ПРЕКУРСОРА

PELIN SÖZEN AKTAŞ

Manisa Celal Bayar University, Faculty of Arts & Sciences, Department of Chemistry, Şehit Prof. Dr. İlhan Varank Campus 45140 Muradiye-Manisa, Turkey

BaTi<sub>5</sub>O<sub>11</sub> се доста испитује захваљујући диелектричним својствима и примени у микроталасним уређајима. Међутим, конвенционалним поступцима се тешко може

добити једнофазни  $\text{BaTi}_5\text{O}_{11}$ . У овом раду је  $\text{BaTi}_5\text{O}_{11}$  синтетисан методом копреципитације коришћењем водених раствора титан(IV)(триетаноламинато)-изопророксида, баријум-нитрата и амонијака као прекурсора који су стабилни у воденој средини. Фазне трансформације током жарења на различитим температурама, фазни састав добијених прахова и структура су испитивани рендгенском дифракционом анализом (XRD), скенирајућом електронском микроскопијом (SEM) енергетском дисперзивном спектроскопијом (EDX). Жељена  $\text{BaTi}_5\text{O}_{11}$  структура једобијена калцинацијом на  $900\text{ }^\circ\text{C}$ . Такође, за карактеризацију су коришћене и термогравиметријска анализа (TGA), инфрацрвена спектроскопија са Фуријеовом трансформацијом (FT-IR) и Раманска спектроскопија. Утврђено је да су честице праха добијеног калцинацијом на  $900\text{ }^\circ\text{C}$  између  $80$  и  $120\text{ nm}$  и да је просечна величина кристалита добијена коришћењем Шерерове формуле  $68,1\text{ nm}$ .

(Примљено 6. јула 2020, ревидирано 10. фебруара, прихваћено 17. фебруара 2021)

#### REFERENCES

1. J. Guo, D. Zhou, H. Wang, X. Yao, *J. Alloys Compd.* **509** (2011) 5863 (<https://dx.doi.org/10.1016/j.jallcom.2011.02.155>)
2. Y. Z. Hao, H. Yang, G. H. Chen, Q. L. Zhang, *J. Alloys Compd.* **552** (2013) 173 (<https://doi.org/10.1016/j.jallcom.2012.10.110>)
3. L. Ren, X. Luo, H. Zhou, *J. Am. Ceram. Soc.* **101** (2018) 3874 (<https://dx.doi.org/10.1111/jace.15694>)
4. C. M. Álvarez-Docio, J. J. Reinoso, G. Canu, M. T. Buscaglia, V. Buscaglia, J. F. Fernández, *Inorg. Chem.* **58** (2019) 8120 (<https://dx.doi.org/10.1021/acs.inorgchem.9b00865>)
5. Y. Higuchi, H. Tamura, *J. Eur. Ceram. Soc.* **23** (2003) 2683 ([https://dx.doi.org/10.1016/S0955-2219\(03\)00193-6](https://dx.doi.org/10.1016/S0955-2219(03)00193-6))
6. S. Tangjuank, T. Tunkasiri, *Mater. Sci. Eng., B* **108** (2004) 223 (<https://dx.doi.org/10.1016/j.mseb.2003.11.022>)
7. C. H. Hsu, W. S. Chen, H. H. Tung, P. C. Yang, J. Sen Lin, *Adv. Mater. Res.* **677** (2013) 153 (<https://dx.doi.org/10.4028/www.scientific.net/AMR.677.153>)
8. H. Zhou, H. Wang, Y. Chen, K. Li, X. Yao, *J. Am. Ceram. Soc.* **91** (2008) 3444 (<https://dx.doi.org/10.1111/j.1551-2916.2008.02623.x>)
9. Y. Chen, E. Li, S. Duan, S. Zhang, *ACS Sustain. Chem. Eng.* **5** (2017) 10606 (<https://dx.doi.org/10.1021/acssuschemeng.7b02589>)
10. V. E. Tillmanns, *Acta Cryst.* **B25** (1969) 1444 (<https://dx.doi.org/10.1107/s0567740869004195>)
11. H. M. O'Bryan, JR., J. Thomson, JR, *J. Am. Ceram. Soc.* **58** (1974) 454 (<https://dx.doi.org/10.1111/j.1151-2916.1975.tb19022.x>)
12. T. Fukui, C. Sakurai, M. Okuyama, *J. Mater. Res.* **7** (1992) 192 (<https://link.springer.com/article/10.1557/JMR.1992.0192#citeas>)
13. S. Li, X. Li, K. Zou, Z. Huang, L. Zhang, X. Zhou, D. Guo, Y. Ju, *Mater. Lett.* **245** (2019) 215 (<https://dx.doi.org/10.1016/j.matlet.2019.02.122>)
14. L. Liu, X. Li, K. Zou, Z. Huang, C. Wang, L. Zhang, D. Guo, Y. Ju, *J. Mater. Sci. Mater. Electron.* **31** (2020) 6883 (<https://dx.doi.org/10.1007/s10854-020-03250-9>)
15. K. Zou, L. Liu, X. Li, S. Li, Z. Huang, L. Zhang, D. Guo, Y. Ju, *Mater. Lett.* **255** (2019) 126584 (<https://dx.doi.org/10.1016/j.matlet.2019.126584>)
16. H. Lu, L. E. Burkhart, G. L. Schrader, *J. Am. Ceram. Soc.* **74** (1991) 968 (<https://dx.doi.org/10.1111/j.1151-2916.1991.tb04329.x>)

17. J. J. Ritter, R. S. Roth, J. E. Blendell, *J. Am. Ceram. Soc.* **62** (1986) 155 (<https://doi.org/10.1111/j.1151-2916.1986.tb04721.x>)
18. S. Tangjuank, L. D. Yu, T. Tunkasiri, *Smart Mater. Struct.* **12** (2003) 656 (<https://doi.org/10.1088/0964-1726/12/4/317>)
19. *Match! - Phase Identification from Powder Diffraction, Crystal Impact - Dr. H. Putz & Dr. K. Brandenburg GbR*, Bonn, Germany, <http://www.crystalimpact.com/match>
20. J. Rodríguez-Carvajal, *Phys., B* **192** (1993) 55 ([https://dx.doi.org/10.1016/0921-4526\(93\)90108-I](https://dx.doi.org/10.1016/0921-4526(93)90108-I))
21. K. Momma, F. Izumi, *J. Appl. Crystallogr.* **41** (2008) 653 (<https://dx.doi.org/10.1107/S0021889808012016>)
22. F. Menges, *Spectragryph - optical spectroscopy software, version 1.2.13*, 2019 (<http://www.effemm2.de/spectragryph>)
23. L. Kong, I. Karatchevtseva, M. Blackford, I. Chironi, G. Triani, *J. Am. Ceram. Soc.* **95** (2012) 816 (<https://dx.doi.org/10.1111/j.1551-2916.2011.05002.x>)
24. J. Javadpour, N. G. Eror, *J. Am. Ceram. Soc.* **71** (1988) 206 (<https://dx.doi.org/10.1111/j.1151-2916.1988.tb05849.x>)
25. Y. Song, F. Wang, Z. Jiang, Y. Zhou, *J. Mater. Sci. Lett.* **18** (1999) 177 (<https://dx.doi.org/10.1023/A:1006699409996>)
26. J. Choy, Y. Han, J. Kim, Y. Kim, *J. Mater. Chem.* **5** (1995) 57 (<https://dx.doi.org/10.1039/JM9950500057>).